LAWRENCE
LIVERMORE
NATIONAL
LABORATORY

UCRL-JRNL-204113

Development of M-shell x-ray spectroscopy and spectropolarimetry of Z-pinch tungsten plasmas

A. Shlyaptseva et al.

April 30, 2004

For submission to Review of Scientific Instruments

DISCLAIMER

Development of M-shell x-ray spectroscopy and spectropolarimetry of Z-pinch tungsten plasmas

A.Shlyaptseva[1], D. Fedin[1], S. Hamasha[1], C. Harris[1], V. Kantsyrev[1], P. Neill[1], N. Ouart[1], U.I. Safronova[1], P. Beiersdorfer[2], K. Boyce[3], G. V. Brown[3], R. Kelly[3], C.A. Kilbourne[3], F. S. Porter[3]

[1]*University of Nevada, Reno*

[2]*Lawrence Livermore National Laboratory*

[3]*NASA Goddard Space Flight Center*

Abstract

The development of spectroscopic modeling of M-shell tungsten z-pinch plasma is presented. The spectral region from 3.5 to 6.5 Å includes three distinct groups of transitions, and the best candidates for M-shell diagnostics are identified. Theoretical modeling is benchmarked with LLNL electron beam ion trap data produced at different energies of the electron beam and recorded by crystal spectrometers and a broadband microcalorimeter. A new high temperature plasma diagnostic tool, x-ray spectropolarimetry, is proposed to study polarization of W line emission and is illustrated using the results of x-pinch polarization-sensitive experiments. The x-ray line polarization of the prominent M-shell tungsten lines is calculated, and polarization markers are identified. The advantage of using x-pinch W wire experiments for the development of M-shell diagnostics is shown.

I. INTRODUCTION

X-pinches are attractive objects for x-ray spectropolarimetry. First, they produce a bright, small x-ray source with a well-defined location that is convenient for experimental measurements. Second, electron beams generated in the plasma produce an observable polarization of the emitted radiation that can be measured. Polarization-sensitive X-pinch experiments have been performed at University of Nevada, Reno (UNR) with Ti [1,2] and Mo [3] X-pinches and will be reviewed later. Also, it was shown that LLNL electron beam ion trap data are extremely helpful in development of the X-ray diagnostics (including x-ray spectropolarimetry) for high temperature and density Z-pinch plasmas [2]. The present work focuses on the development of X-ray spectroscopy and spectropolarimetry for M-shell W plasmas. This plasma is a very challenging object for diagnostics because of contributions from numerous ionization stages in a narrow spectral region that are impossible to resolve. Ion trap measurements will allow us to break down this very complicated M-shell spectrum into spectra produced by separate W ions and will benchmark advanced atomic physics calculations. Experimental and theoretical spectra are presented and analyzed in Section II. X-ray spectropolarimetry of x-pinch experiments is discussed in Section III.

II. EXPERIMENTAL AND THEORETICAL X-RAY M-SHELL W SPECTRA

M-shell W spectra produced at the LLNL EBIT-I and EBIT-II electron beam ion traps have been collected in two different experiments using an X-ray crystal spectrometer (Fig. 1) and an engineering model X-Ray Spectrometer (XRS) microcalorimeter (Fig. 2). The operation of the LLNL ion traps and their numerous

applications and advantages are described in detail elsewhere (see, for example, [4]). Both M-shell W spectra have been produced at the energy of the electron beam E_b=3.9 keV. In particular, Fig. 1 shows the spectrum recorded by a crystal spectrometer in a previous experiment on EBIT-II, which was described in [5]. This spectrometer covered a spectral range from 5 to 6 Å with a spectral resolution of 2200. Three Ni-like lines dominate this spectral region and will be discussed in the next section. Figure 2 shows a newly recorded spectrum using the XRS.

The flight model XRS microcalorimeter is scheduled to be put into orbit next February as part of the Astro-E2 mission [6]. The engineering model XRS microcalorimeter, as fielded on EBIT-I, is capable of acquiring, filtering and characterizing x-ray events on 32 independent pixels, as described by Porter et al. in these Proceedings. Though designed with modest imaging capability for the Astro-E2 mission, no x-ray imaging was employed on EBIT-I. In the present measurements, only 14 pixels were used. These function simply as 14 independent non-dispersive x-ray spectrometers. The XRS detects x-rays from below 400 eV to above 10 keV with high quantum efficiency and a resolution of about 6 eV at 6 keV. Wavelength calibration is built into the data acquisition system, but there is some residual drift that must be taken into account at run time. This was accomplished using EBIT-I itself by injecting calibration gases and using the known energies of F, Ne, S, and Cl K shell emissions in a 3rd order polynomial fit. Tungsten was injected into the trap in low charge states by a Metal-Vapor Vacuum Arc (MeVVA) subsystem mounted on the axis of the electron beam. A seven-second EBIT injection/trap/dump timing cycle was synchronized to the XRS data stream, and each x-ray event was tagged with its phase in the cycle. This allowed data from the

first second of each timing cycle, when low charge states were present, to be discarded. The spectrum shown in Fig. 2 is from a single pixel (there are 13 more) with an effective integration time of 105 minutes. The XRS has the advantages of high-count rate (considerably higher than that of crystal spectrometers) and broadband spectral coverage. In addition, XRS is insensitive to the individual polarization components. In contrast, crystal spectrometers have greater resolution and preferentially reflect one polarization component. The complementary aspects of the two spectrometer types will be put to use in making polarization measurements using the present data set.

In Fig. 2, the most intense and diagnostically important M-shell spectral features are labeled. They are the Ni-like lines, specifically Ni1 ($3p^6 3d^9 4f\ ^1P_1$- $3p^6 3d^{10}\ ^1S_0$), Ni2 ($3p^6 3d^9 4f\ ^3D_1$- $3p^6 3d^{10}\ ^1S_0$), Ni3 ($3p^5 3d^{10} 4d\ ^1P_1$- $3p^6 3d^{10}\ ^1S_0$), Ni4 ($3p^5 3d^{10} 4s\ ^3D_1$- $3p^6 3d^{10}\ ^1S_0$), Ni5 ($3p^6 3d^9 5f\ ^1P_1$- $3p^6 3d^{10}\ ^1S_0$), Ni6 ($3p^6 3d^9 5f\ ^1P_1$- $3p^6 3d^{10}\ ^1S_0$), Ni7 ($3p^5 3d^{10} 4d\ ^3P_1$- $3p^6 3d^{10}\ ^1S_0$), Ni8 ($3p^6 3d^9 6f\ ^1P_1$- $3p^6 3d^{10}\ ^1S_0$) and Ni9 ($3p^6 3d^9 6f\ ^1P_1$- $3p^6 3d^{10}\ ^1S_0$). These lines form three groups of transitions. In particular, the first four lines are due to 3-4 transitions, the next two lines are due to 3-5 transitions, and the last two are due to 3-6 transitions. The idea of the use of the XRS was to provide a broadband spectrum (from 3 to 6.5 Å in this case), which includes all three groups of transitions important for HED plasma diagnostics. We develop the model that can describe the XRS spectrum as a benchmark but can be also very useful for HED plasma diagnostic. For comparison, the spectrum for the crystal spectrometer covers only from 5 to 6 Å (Fig. 1), which includes only one group of transitions. Also, insensitivity of the XRS to polarization is a very important advantage.

In Fig. 3, a synthetic spectrum of M-shell W was calculated using a non-LTE kinetic program with a monoenergetic electron beam at E_b=3.9 keV for the spectral region from 3.5 Å to 6.5 Å. The W kinetic model used in this paper is described in detail in [7]. Figure 3 shows that Ni-like lines dominate at this electron energy (the average charge <Z>=45.8). In general, theory (see Fig. 3) agrees well with experiment (see Figs. 1 and 2). The one exception is the intensity of line Ni7. The same model can be applied to study x-ray radiation from high temperature and density W plasmas. For example, synthetic spectra of M-shell W calculated for Maxwellian plasmas at the electron density 10^{21} cm^{-3} indicate the prominence of the same Ni-like lines (Ni1-Ni9) in a broad plasma temperature range from 1.4 to 2.0 keV. In particular, the intensity ratio of Ni5 and Ni6 is very sensitive to the changing of plasma parameters and serve as a sensitive temperature diagnostic.

III. X-PINCH X-RAY SPECTROPOLARIMETRY

Polarization-sensitive experiments were performed on the 1 MA pulse power Z-pinch device for Ti and Mo X-pinches. Polarization-sensitive Ti X-pinches have been analyzed earlier [1,2], whereas recently the first analysis of polarization-sensitive Mo X-pinches was presented [3]. In these spectrometers the two-crystal technique was implemented to detect line polarization [8]. Specifically, for both types of X-pinches, polarization-sensitive spectra have been collected by two identical convex crystal spectrometers with Bragg angle close to 45^o in such a way that one spectrometer was recording an almost pure parallel polarization state (spectrometer H) whereas the other one was recording an almost pure perpendicular polarization state (spectrometer V). The

difference in simultaneously recorded H and V traces infers information about polarization of lines and then about the presence of electron beams in plasmas. Analysis of Ti and Mo X-pinch polarization-sensitive experiments indicate x-ray line polarization in two Ti and three Mo shots. The scheme of a diagnostic setup (used in Ti and Mo experiments) has been modified and is presented in Fig. 4. This scheme includes 2D (previously 1D) polarimeter/spectrometers with concave spherical crystals (previously flat crystals). This diagnostic setup is planned for use in polarization-sensitive W experiments.

In Fig. 5, theoretical values of the degree of polarization for the most prominent He-like Ti lines and Ni-like W lines is calculated for different energies of electron beams in threshold units using the newly developed, relativistic, multiconfigurational atomic package by M.F. Gu [9]. The excitation thresholds for these lines vary from 2 keV to 3.3 keV for Ni-like W lines up to 4.75 keV ($w=1s2p\,^1P_1 \rightarrow 1s^2\ ^1S_0$) and 4.73 keV ($y=1s2p\,^3P_1 \rightarrow 1s^2\ ^1S_0$) for He-like Ti lines. Figure 5 demonstrates that despite of the very different origin and properties of K-shell Ti and M-shell W lines they have similar polarization properties, and we can use similar techniques in study of polarization of M-shell lines. In particular, Ni-like W lines form three groups: the first group with higher polarization (45-55 % near threshold), which includes lines Ni3 and Ni4; the second, middle group with lower polarization than the first group (25-35% near threshold, lines Ni1 and Ni2), and the third group with the lowest polarization (25-35 % near threshold but then decreasing more rapidly), which includes lines Ni5, Ni6, Ni8, and Ni9. Relatively high polarizations at the threshold and the prominent difference in polarization of these groups can be useful in future spectropolarimetry studies.

ACKNOWLEDGMENTS

Research supported by DOE-NNSA/NV Cooperative Agreement DE-FC08-01NV14050, LLNL and SNL. Work by the University of California Lawrence Livermore National Laboratory was performed under the auspices of the U.S. DOE under contract W-7405-Eng-48.

REFERENCES

1. A.S. Shlyaptseva, S.B. Hansen, V.L. Kantsyrev, B.S. Bauer, D.A. Fedin, N. Ouart, S.A. Kazantsev, A.G. Petrashen, U.I. Safronova, *Rev. Sci. Instr*. **72**, 1241, 2001.

2. A.S. Shlyaptseva, D.A. Fedin, S.M. Hamasha, S.B. Hansen, C. Harris, V.L. Kantsyrev, P. Neill, N. Ouart, P. Beiersdorfer, U.I. Safronova, *Rev. Sci. Instr*. **74**, 1947, 2003.

3. A.S. Shlyaptseva, V.L. Kantsyrev, N. Ouart, D. Fedin, S. Hamasha, S. Hansen, *Proceedings of SPIE* **5196**, 16 (2004).

4. P. Beiersdorfer, J.A. Britten, G.V. Brown *et al*, Physica Scripta T92, 268 (2001).

5. P. Neill, C. Harris, A.S. Shlyaptseva, S. Hamasha, S. Hansen, P. Beiersdorfer, U.I. Safronova, University of California Report No. UCRL-JRNL-201473 (2003).

6. http://lheawww.gsfc.nasa.gov/docs/xray/astroe/astroe.html

7. S. Hamasha. PhD Dissertation, University of Nevada, Reno (Jan. 2004).

8. P. Beiersdorfer, D.A. Vogel, K.J. Reed, V. Decaux, J.H. Scofield, K. Widmann, G. Hölzer, E. Förster, O. Wehrhan, D.W. Savin, L. Schweikhard, *Phys. Rev. A* **53**, 3974, 1996.

9. M.F. Gu, *Astropys. J.* **582**, 1241, 2003.

FIGURE CAPTIONS

Fig. 1. Experimental M-shell W spectrum from the LLNL EBIT-II recorded by the crystal spectrometer at E_b=3.9 keV.

Fig. 2. Experimental M-shell W spectrum from the LLNL EBIT-I recorded by the XRS microcalorimeter at E_b=3.9 keV.

Fig. 3. Theoretical synthetic spectrum calculated for Gaussian electron distribution function centered at 3.9 keV.

Fig. 4. Experimental setup for polarization-sensitive measurements in X-pinch experiments.

Fig. 5. Polarization of the most prominent He-like Ti and Ni-like lines of W as a function of the electron beam energy in threshold units.

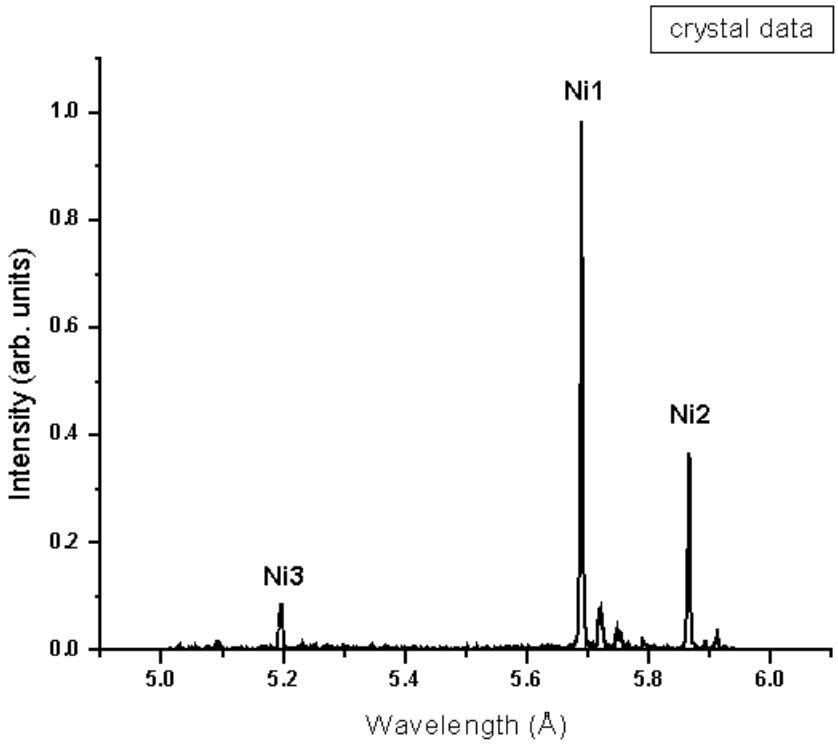
crystal data
Ni1
Ni2
Ni3
Intensity (arb. units)
Wavelength (Å)
0.0
0.2
0.4
0.6
0.8
1.0
5.0
5.2
5.4
5.6
5.8
6.0

Fig.1

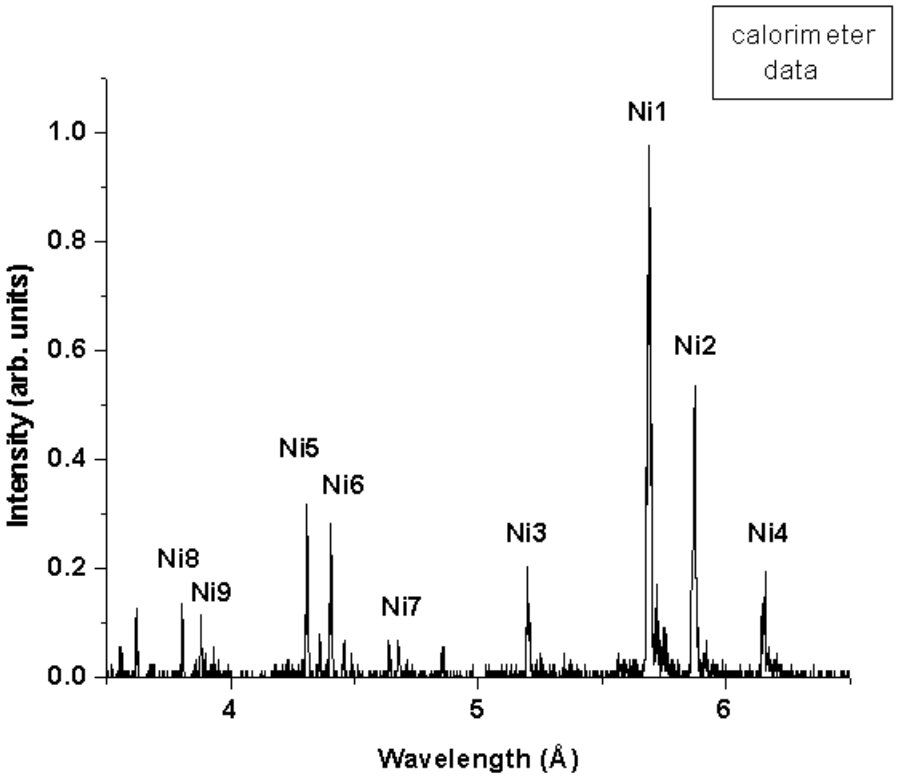
calorimeter data
Ni1
Ni2
Ni3
Ni4
Ni5
Ni6
Ni7
Ni8
Ni9
Intensity (arb. units)
Wavelength (Å)
0.0
0.2
0.4
0.6
0.8
1.0
4
5
6

Fig.2

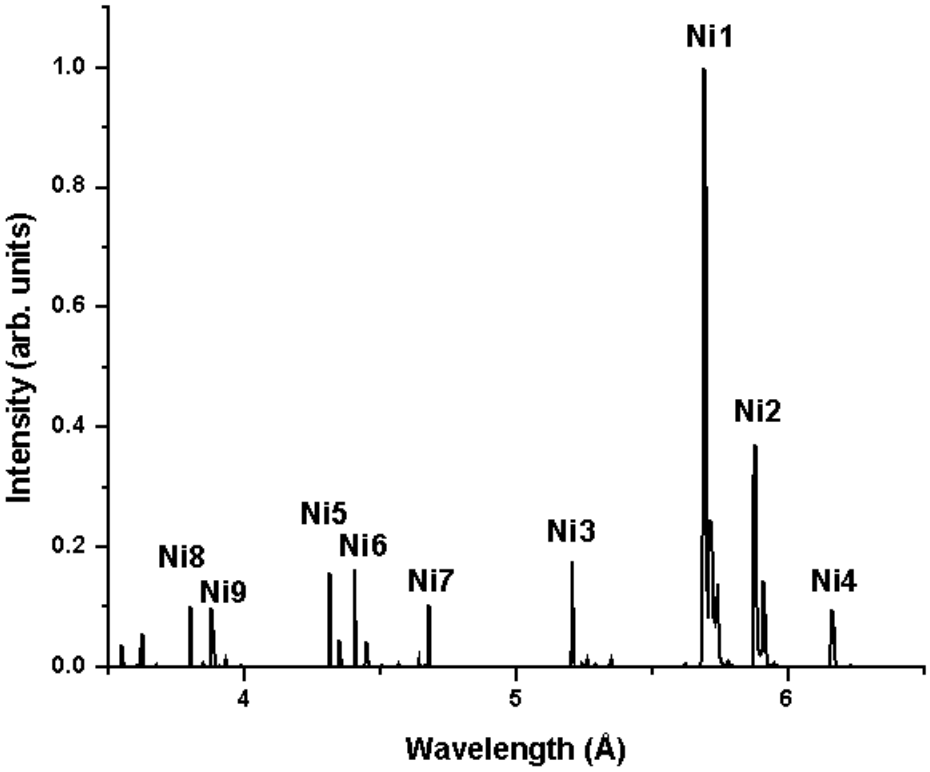
Ni1
Ni2
Ni3
Ni4
Ni5
Ni6
Ni7
Ni8
Ni9
Intensity (arb. units)
Wavelength (Å)
0.0
0.2
0.4
0.6
0.8
1.0
4
5
6

Fig.3

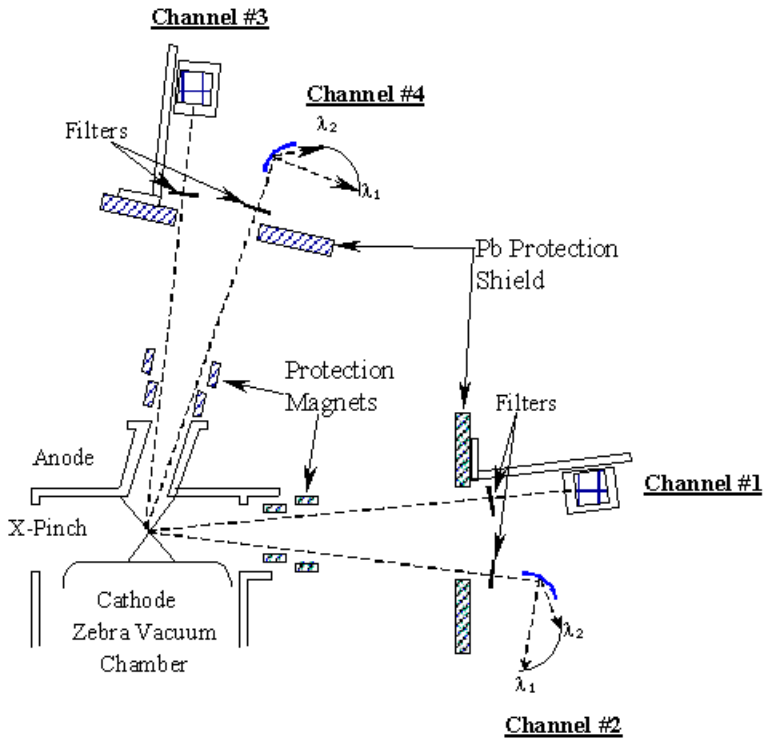
Channel #3
Channel #4
Filters
λ2
λ1
Pb Protection
Shield
Protection
Magnets
Filters
Anode
Channel #1
X-Pinch
Cathode
Zebra Vacuum
Chamber
λ2
λ1
Channel #2

Fig.4

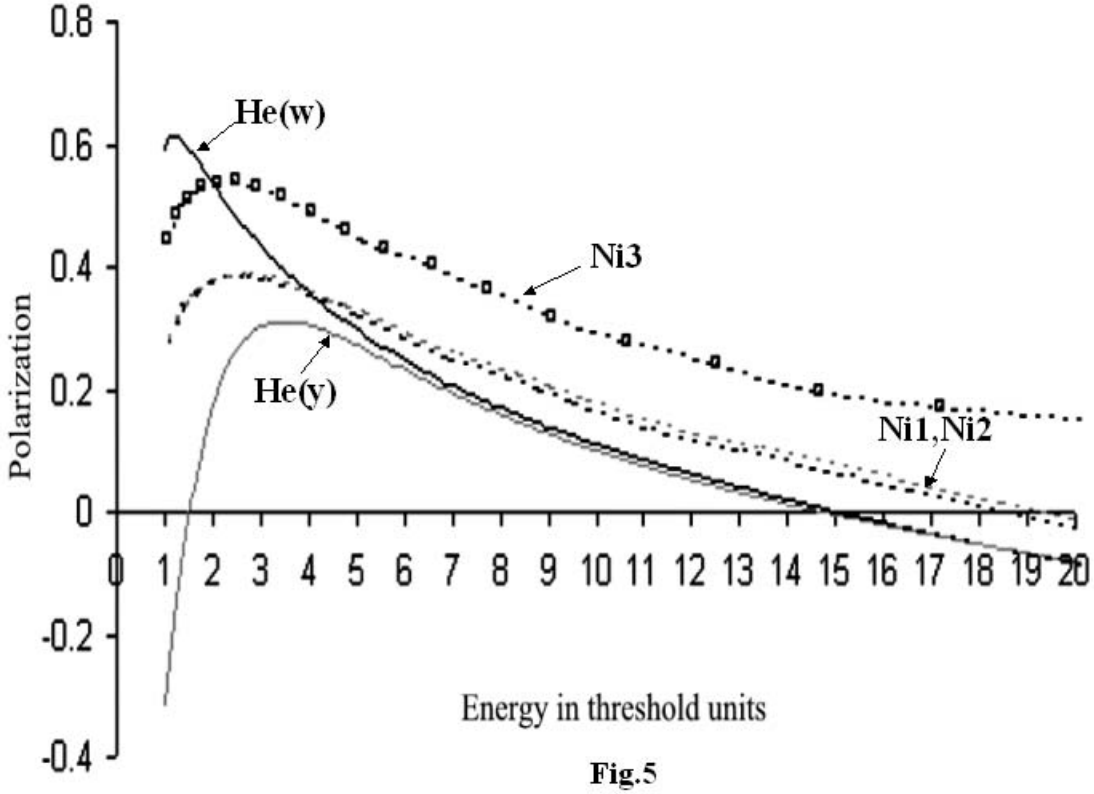
0.8
0.6
0.4
0.2
0
-0.2
-0.4
Polarization
He(w)
Ni3
He(y)
Ni1,Ni2
0 1 2 3 4 5 6 7 8 9 10 11 12 13 14 15 16 17 18 19 20
Energy in threshold units

Fig.5

University of California
Lawrence Livermore National Laboratory
Technical Information Department
Livermore, CA 94551